PHYSICAL REVIEW B

CONDENSED MATTER

THIRD SERIES, VOLUME 29, NUMBER 1 1 JANUARY 1984

Evidence for isoelectronic Sn for Ge substitution in crystalline and glassy $GeSe_2$

P. Boolchand and Mark Stevens

Physics Department, University of Cincinnati, Cincinnati, Ohio 45221

(Received 11 August 1983)

Ternary alloy glasses $Ge_{1-x}Sn_xSe_2$ in the low-Sn-concentration range $0.002 < x < 0.010$ have been prepared and crystallized by heating to the crystallization temperature T_{cryst}. Mössbauer spectroscopy is used to follow changes in bonding chemistry of the Sn dopant on crystallization of the glasses. Polymorphous crystallization of these Sn-poor glasses leads to the formation of tetrahedral Sn as in $Sn(Se_{1/2})_4$ local unit and octahedral Sn as in a c-SnSe phase but not as in a c-$SnSe_2$ phase. The latter crystalline phase is found when sputtered amorphous $SnSe_2$ films are crystallized. The tetrahedral Sn site observed in the glasses, as in the corresponding crystals, can therefore not come from an amorphous Sn-rich tetrahedral $SnSe_2$ phase but must come from Sn replacing Ge sites in a tetrahedral $GeSe_2$ phase. A lower limit to the solubility of Sn at Ge in c-$GeSe_2$ is placed at 0.2 at. % while in the glasses it is substantially larger and is conservatively placed at 3 at. %. These results demonstrate that the two sites provide evidence for broken chemical order in g-$GeSe_2$.

I. INTRODUCTION

In a previous paper[1] we examined the microscopic origin of broken chemical order in a $GeSe_2$ glass using ^{119}Sn Mössbauer spectroscopy. In our interpretation of the data we assumed that according to the $8-N$ rule, Sn replaces available Ge sites of the network, i.e., isoelectronic substitution occurs. Alternatively, Sn could phase separate in a tetrahedral $SnSe_2$-rich phase. Since this question is of central importance in the interpretation of the Mössbauer data, and furthermore, since the conclusions from that work dwell centrally on the network morphology of $GeSe_2$, we have examined the Sn-bonding configuration in this glass in some detail in this paper.

Our approach is to examine the crystallization process of ternary alloy glasses $Ge_{1-x}Sn_xSe_2$ for low Sn concentrations $x=0.002$, 0.004, and 0.010, and to compare this behavior to the case of an amorphous $SnSe_2$ film. The glasses were prepared in the usual way by melt quenching in water and were crystallized by heating in vacuum for 15 min at $T_{cryst}=480\,^{\circ}C$, the crystallization temperature.[2] Changes in the Sn-bonding chemistry were followed using Mössbauer spectroscopy principally. It will be shown in this work that the spectra provide compelling evidence for isoelectronic substitution of Sn at Ge sites in both $GeSe_2$ glass and crystal. A lower limit to the solubility of Sn in the crystal is placed at 0.2 at. %, whereas in the glass the solubility is substantially higher and is placed conservatively at 3 at. %. The present results on the $Ge_{1-x}Sn_xSe_2$ system are strikingly different from those found on the $Si_{1-x}Ge_xS_2$ system. In the latter, evidence[3] for molecular phase separation is found in both the glassy and crystalline phases. These diverse spectroscopic results bring up the following question: Under what conditions does a supercooled ternary $A_XB_{1-x}X_2$ melt choose isoelectronic substitution $(A,B)X_2$ over phase separation $(AX_2)_x(BX_2)_{1-x}$? We address this question in the concluding section of this paper.

In Sec. II we present the experimental results. In Sec. III we identify the microscopic nature of Sn sites from the nuclear hyperfine structure. In Sec. IV we correlate this information with cluster morphology and comment on the dopant solubility in both c- and g-$GeSe_2$. We conclude our discussion with Sec. V, where we outline general conditions that favor isoelectronic substitution over molecular phase separation in a supercooled melt.

II. EXPERIMENTAL RESULTS

The principal results of the present work are summarized in Figs. 1 and 2. These figures display, respectively, spectra of $Ge_{1-x}Sn_xSe_2$ glasses and crystals taken as a function of Sn-dopant concentration x. One immediately recognizes from these figures that while the shape of spectra in the crystals change drastically with x, just the reverse happens for the case of glasses, i.e., the shape of the spectra remain independent of x. We have analyzed[4] these spectra in terms of two Sn sites: A site labeled A that shows a single line centered near $+1.55$ mm/s and a second site that exhibits a partially resolved doublet with a

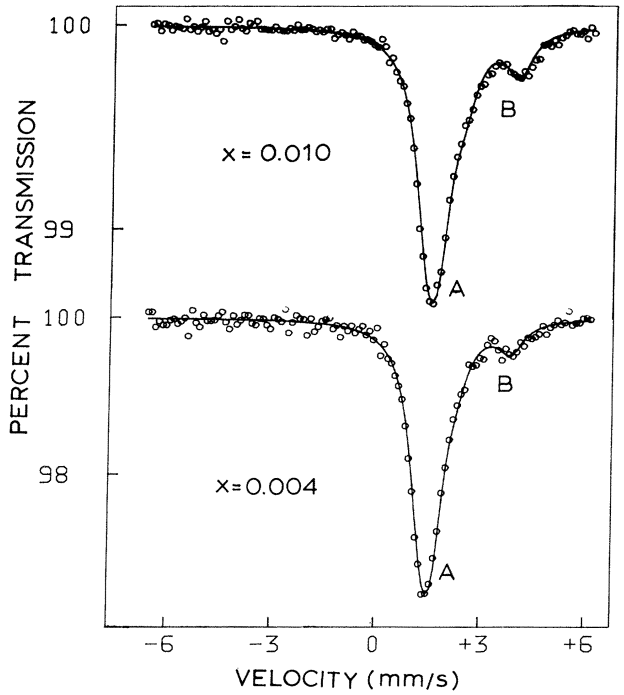

FIG. 1. Spectra of $Ge_{1-x}Sn_xSe_2$ glasses showing evidence for broken chemical order. The two sites are site A, the intense narrow line and site B, the weak quadrupole doublet. These spectra show that the site intensity ratio $I_B/(I_A+I_B)$ is independent of x for the two compositions studied. See Fig. 5 and text for further details.

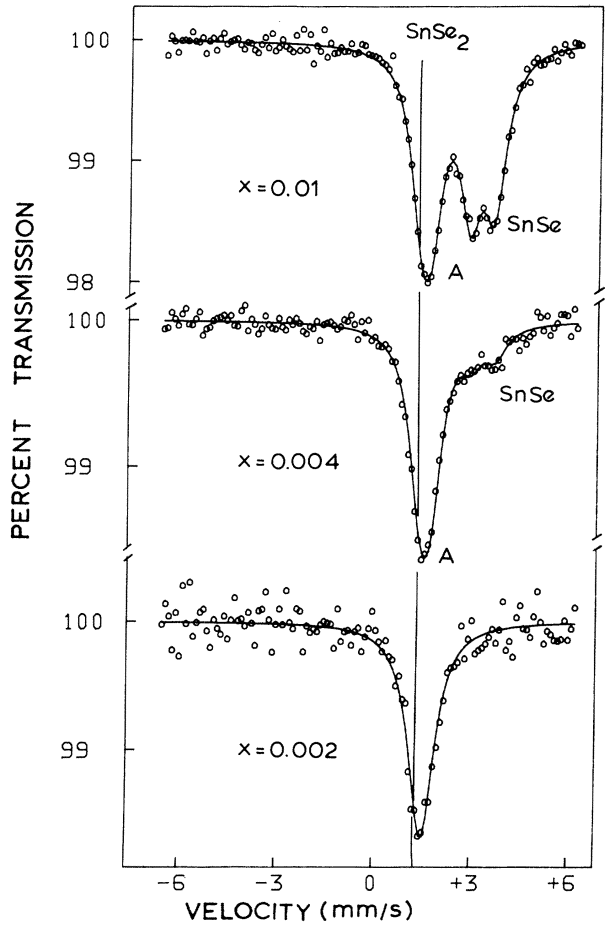

FIG. 2. Spectra of $Ge_{1-x}Sn_xSe_2$ crystals obtained from crystallization of corresponding glasses, showing phase separation of c-SnSe phase with increasing x. Site A is identified with Sn replacing tetrahedrally coordinated Ge in the layered structure of $GeSe_2$. For reference purposes, we have also shown by a vertical line the isomer shift of c-$SnSe_2$. Also see Fig. 5.

centroid near $+3.2$ mm/s. These spectra were taken using a $^{119}Sn^m$ source in $CaSnO_3$. The source and absorber were cooled to 78 K in a system described elsewhere.[1]

Following standard procedures of data analysis[4] we obtained isomer shifts δ and quadrupole splittings Δ of the two sites seen in both glasses and crystals. These data are summarized in Table I. For reference purposes we have included in this table Mössbauer parameters for certain well-characterized, crystalline Sn environments. In the next section we proceed to identify the microscopic nature of these sites from the measured nuclear hyperfine structures.

III. DISCUSSION

In covalent materials, in contrast to metallic or ionic hosts, the nuclear hyperfine structure is largely determined[5] by the distribution of $5s$ and $5p$ valence electrons of Sn. It is for this reason that the δ and Δ parameters provide a microscopic fingerprint of the Sn local environment. Specifically, the δ parameter probes the contact electron density $|\psi(0)|^2$ at the Sn nucleus, measured relative to some reference host (usually Sn^{4+} as in SnO_2 or $CaSnO_3$), through the usual relation

$$\delta=(2\pi/5)Ze^2\Delta\langle r^2\rangle[\,|\psi(0)|^2-|\psi(0)|^2_{\rm ref}]\,, \qquad (1)$$

while the Δ parameter measures the asphericity of the $5p$ charge distribution through the EFG tensor (V_{zz}, $\eta=|(V_{xx}-V_{yy})/V_{zz}|$) and is given by the relation

$$\Delta=\tfrac{1}{2}e^2QV_{zz}(1+\eta^2/3)^{1/2}\,. \qquad (2)$$

We note that the δ and Δ parameters (Table I) of site A seen in $Ge_{1-x}Sn_xSe_2$ glasses and crystals are identical. On this basis, we conclude that the microscopic nature of this site in both crystals and glasses is the same.

A. Nature of site A in crystals and glasses of $Ge_{1-x}Sn_xSe_2$

Before actually proceeding to identify the nature of site A from the nuclear hyperfine structure, it may be well worth excluding certain obvious possibilities. It is seen from Table I and Fig. 3 that the δ and Δ parameters of site A, while close to those of Sn substitutional in c-Ge or of c-$SnSe_2$, are nevertheless measurably different. In Fig. 3 we show spectra of c-$SnSe_2$ and c-$Ge_{0.99}Sn_{0.01}Se_2$. Both of these spectra were recorded in our spectrometer using the same conditions for comparison purposes. We note that not only is the linewidth of the c-$SnSe_2$ resonance (bottom spectrum) narrower, but this resonance is actually shifted by -0.2 mm/s with respect to site-A resonance

TABLE I. ^{119}Sn isomer shift (δ), quadrupole splitting (Δ), and full width at half maximum (Γ_{obs}) in indicated crystalline (c) and glass (g) samples. All measurements were performed at 78 K.

Sample	Site	δ[a] (mm/s)	Δ (mm/s)	Γ_{obs} (mm/s)	Reference
c-$Ge_{1-x}Sn_xSe_2$[b]	A	1.55(2)	0.35(2)	0.82(7)	Present work;
	Sn^{2+}	3.33(13)	0.74(4)	0.82(7)	also see Ref. 1
g-$Ge_{1-x}Sn_xSe_2$[b]	A	1.55(2)	0.33(4)	0.82(4)	Present work;
	Sn^{2+}	3.12(15)	1.57(10)	0.82(3)	also see Ref. 1
Sn in g-Se		1.69(2)	~0	0.82(2)	Present work
c-$SnSe_2$		1.36(2)	~0		Ref. 9
c-SnSe		3.31(2)	0.74(2)	0.89(4)	Ref. 10
Sn in c-Ge		1.97(6)	~0		Ref. 16
c-SnO	Black form	2.69(2)	1.33(1)	0.85(2)	Ref. 17
	Red form	2.60	2.20		Ref. 18
c-SnO_2		~0	c		Ref. 19

[a]Shifts are quoted relative to $CaSnO_3$.
[b]The δ and Δ parameters are independent of x for the three concentrations $x=0.002$, 0.004, and 0.01 examined in this work.
[c]Stoichiometry dependent.

(top spectrum). These results are in excellent agreement with published shifts (Table I) of these resonances. On this basis we exclude the possibility that site A represents octahedral Sn in a c-$SnSe_2$ (CdI_2) layered morphology.

We suggest that site A represents Sn that is tetrahedrally coordinated to four Se near neighbors in a local tetrahedral $Sn(Se_{1/2})_4$ unit. In support of this claim we point out that the shift δ of this site forms part of a systematic trend that is observed for isostructural SnX_4 tetrahedral species.

In Fig. 4, we have plotted the δ of a variety of SnX_4 species as a function of the Pauling electronegativity difference $\Delta\chi_p=\chi_X-\chi_{Sn}$. The linear correlation found between δ and $\Delta\chi_p$ has the following physical interpretation. Starting from α-Sn (diamond cubic structure), which represents Sn in a sp^3 valence configuration, the ef-

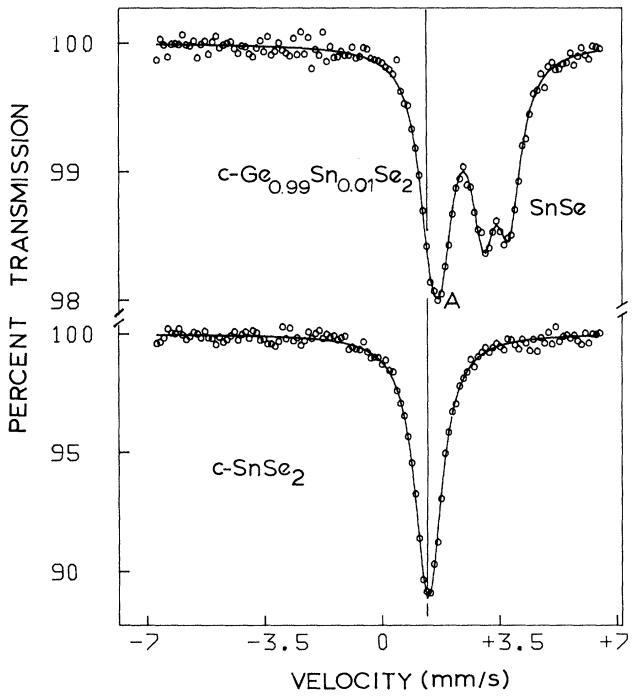

FIG. 3. Comparison of spectra of indicated crystals taken under similar conditions. The small but measurable shift of -0.20 mm/s of c-$SnSe_2$ with respect to the site-A resonance in c-$Ge_{0.99}Sn_{0.01}Se_2$ indicates that the latter site does not represent octahedral Sn. This is, in fact, shown to be tetrahedral Sn. See Fig. 4 and text for further details.

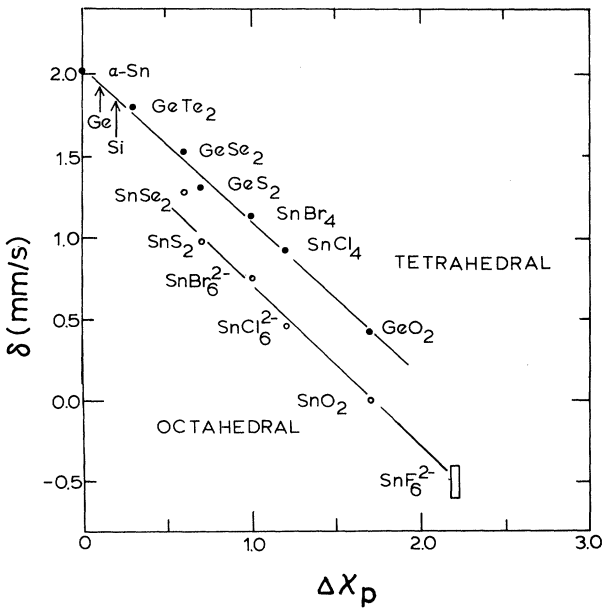

FIG. 4. Plot of isomer shift δ as a function of $\Delta\chi p=\chi(X)-\chi(Sn)$ for isostructural tetrahedral SnX_4 local units. $\chi(X)$ represents the Pauling electronegativity of atom X. The justification of this linear correlation is discussed in text and the Appendix. The shifts for GeX_2 (X=O,Se,Te) are taken from our glass work, while shifts for α-Sn, $SnBr_4$, and $SnCl_4$ are taken from Ref. 19. For comparison purposes we have also shown δ for corresponding octahedral SnX_6 species and find these shifts to be systematically less positive. This is attributed to the shielding of two additional $5d$ electrons as one goes from a sp^3 hybrid (tetrahedral) to a sp^3d^2 hybrid (octahedral).

fect of replacing Sn by a more electronegative ligand (X) in that local tetrahedral geometry is to remove some of the sp^3-like charge from the covalent bond to the ligand. This lowers the contact charge density $|\psi(0)|^2$ (mainly due to $5s$ electrons) and therefore reduces δ [Eq. (1)] in proportion to $\Delta\chi_p$. The slope of the line on this plot, when transformed to the appropriate charge unit (see the Appendix), yields a value of $0.21e$ per unit $\Delta\chi_p$. It is remarkable that this value is in excellent agreement with the value suggested[6] by Pauling in 1942 when he first introduced the concept of atomic electronegativities.

It is important to recognize that the lack of any significant Δ is an independent experimental fact that supports the tetrahedral character of site A. To a first approximation, since the $5p_x$, $5p_y$, and $5p_z$ valence orbitals of Sn are equally populated ($U_x=U_y=U_z$) in a sp^3 hybrid orbital, the net electric-field gradient (EFG),

$$V_{zz}=\frac{-4e}{5\langle r^3\rangle}\left[U_z-\frac{U_z+U_y}{2}\right], \tag{3}$$

vanishes. Following Eq. (2), the quadrupole splitting Δ also vanishes. The small but finite value of Δ for site A in both the crystals and glasses is interesting and will be discussed elsewhere.

B. Nontetrahedral site in $Ge_{1-x}Sn_xSe_2$ crystals

In the Sn-poor crystals, we identify the partially resolved doublet with phase-separated c-SnSe clusters. This identification is based on the fact that the Mössbauer parameters (δ,Δ) of this site are identical to those found for c-SnSe (Table I). In this crystal Sn is described as Sn^{2+} and it possesses a distorted octahedral coordination in a three-dimensional morphology. This interpretation of the Mössbauer data is in harmony with x-ray diffraction results on a crystalline $Ge_{0.99}Sn_{0.004}Se_2$ sample that reveals Bragg peaks corresponding to orthorhombic SnSe and crystalline $GeSe_2$.

We have also investigated[7] the crystallization behavior of a sputtered amorphous $SnSe_2$ film and have found that the principal phase to emerge at $T_{\text{cryst}}\cong 210\,^\circ\text{C}$ is c-$SnSe_2$. Thus, the crystallization behavior of Sn-poor and Sn-rich alloy glasses leads to different crystalline phases. This is a point we will return to later in Sec. IV A.

C. Nontetrahedral site in $Ge_{1-x}Sn_xSe_2$ glasses

It is at once clear from the data of Table I that the nontetrahedral site seen in $Ge_{1-x}Sn_xSe_2$ glasses has δ and Δ parameters that are sufficiently different from those found in corresponding crystals, so that this site cannot be identified with Sn present in c-SnSe phase. The site in question was identified by us earlier[1,8] as arising from Sn replacing Ge in a quasi-one-dimensional, Ge-rich cluster of Ge_2Se_3 stoichiometry (i.e., a Ge—Ge pair is replaced by a Ge—Sn pair, each Ge and Sn still having three Se near neighbors).

This identification was based on the composition dependence of site intensity ratios in Sn-doped $Ge_{1-x}Se_x$ glasses, and the reader is referred to the extensive discussion of this point in Refs. 1 and 8. In this quasi-tetrahedral geometry, Sn apparently chooses to be in a Sn^{2+} state (as shown by δ) and we suggest that this is a strain minimization mediated by atomic size considerations. Because the covalent radius[6] of Sn (1.41 Å) is substantially larger than its divalent one (1.12 Å), and furthermore, because the latter is more compatible with the covalent radius of Ge (1.22 Å), the strain energy associated with tetrahedral face sharing of the doped cluster can apparently be minimized by the dopant choosing its Sn^{2+} state in this quasi-one-dimensional cluster.

IV. CRYSTALLIZATION PROCESS AND DOPANT SOLUBILITY

Having identified the microscopic nature of various Sn sites, we can now comment on the crystallization process of glasses, the cluster morphologies involved, and the dopant solubility.

A. Isoelectronic substitution and solid solubility of Sn at Ge in c-$GeSe_2$

In the present ternary, the crystallization behavior of Sn-poor glasses ($x\approx 0$) is in sharp contrast to the behavior seen for Sn-rich glasses ($x\cong 1$). In the latter glasses, primary crystallization leads to the formation[7] of a c-$SnSe_2$ phase. Apparently, when a Sn-rich tetrahedral $SnSe_2$ phase is present, as it is in sputtered amorphous $SnSe_2$,[7] crystallization leads to an increase in Sn coordination from 4 to 6, to form the corresponding crystal of the same stoichiometry.

This is clearly not the situation for the Sn-poor glasses, where as described in Sec. III B, crystallization leads to tetrahedral Sn (site A) and c-SnSe but not octahedral Sn as in c-$SnSe_2$.[9] This is suggestive of the fact that the Sn dopant is not present in a Sn-rich, phase separated, tetrahedral $Sn(Se_{1/2})_4$ cluster, as is found in amorphous $SnSe_2$. It is on this basis that we ascribe site A to Sn, replacing Ge in a tetrahedral $GeSe_2$ network. One may also understand the rapid increase in the c-SnSe fraction with x shown in Fig. 1, as follows. We show in Fig. 5 a plot of the site intensity ratio of $I(\text{SnSe})/I(A)$ from the spectra of Fig. 1. The observation of site A only at $x=x_l=0.002$ constitutes a lower limit to the solubility x_l of Sn for Ge in the layered structure of c-$GeSe_2$. For $x>x_l$, further isoelectronic substitution is apparently hindered on account of strain (the covalent radius of Sn is 15% larger than Ge), and the additional Sn (nearly all of it) is driven out of the $GeSe_2$ layered morphology, and segregates in pockets of c-SnSe phase[10] (a distorted NaCl phase). The crystallization process results in locally increasing the Sn coordination from 4 to 6, thereby compacting the network and recovering the 10% density deficit that usually exists between glasses and crystals.

B. Sn-bonding chemistry in g-$GeSe_2$

Perhaps the most significant result to emerge from the present work is the constancy of I_B/I (see Figs. 2 and 5) at low x. Experiments on alloys containing higher concentrations ($0.01<x<0.50$) of Sn indicate that I_B/I

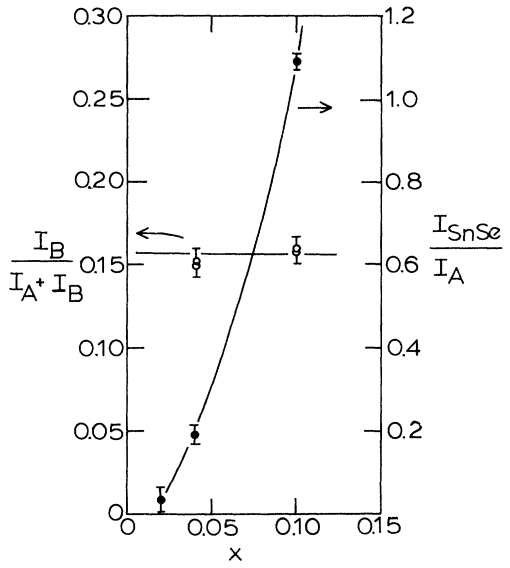

FIG. 5. x variation of I_B/I and I_{SnSe}/I_A for $Ge_{1-x}Sn_xSe_2$ glasses and crystals deduced from spectra of Figs. 1 and 2, respectively. The constancy of I_B/I indicates that $x=0.01$ represents the dilute limit. The rapid increase of I_{SnSe}/I_A with x indicates that phase separation of c-SnSe occurs when $x > 0.002$, the solubility limit of Sn for Ge sites in c-$GeSe_2$.

remains at 0.16 for values of x as large as 0.03. This indicates that apparently substantial isoelectronic substitution (Sn for Ge) can take place in the molecular structure of $GeSe_2$ without detectable modification of this structure. This view is also supported by Raman spectra[11] of $Ge_{1-x}Sn_xSe_2$ glasses, which indicate that local vibrational modes of $Sn(Se_{1/2})_4$ tetrahedral units appear with increasing x. The first clear indication of substantial degradation of molecular structure appears when $x \cong 0.15$, and this is discussed in detail in Refs. 11 and 12. Because of a spread in bond angles and bond lengths, it is reasonable to expect a higher degree of isoelectronic substitution to occur in glasses than in crystals. In glasses the attendant strain associated with an undersized or oversized dopant can be locally relieved instead of being propagated over a few lattice sites, as it would in a crystal.

C. Broken chemical order in g-$GeSe_2$

The singularly most important consequence of the present work is to demonstrate that the broken chemical order[1] in $GeSe_2$ glass is an intrinsic property of the glass network. This broken order is neither the consequence of insufficient dopant solubility at tetrahedral $Ge(Se_{1/2})_4$ sites of the network nor is it the result of a phase-separated Sn-rich $SnSe_2$ tetrahedral phase coexisting with a $GeSe_2$ tetrahedral phase in these glasses. Indeed, the former is excluded by the constancy of I_B/I as $x \to 0$, while the latter is ruled out from the absence of a c-$SnSe_2$ phase in the $Ge_{1-x}Sn_xSe_2$ samples upon crystallization, as discussed previously in Sec. IV A. The microscopic origin of this broken chemical order, as discussed earlier,[1] is the consequence of at least two types of morphologically distinct, immiscible clusters that are present in the stoichiometric glass.

V. ISOELECTRONIC SUBSTITUTION VERSUS PHASE SEPARATION IN SUPERCOOLED PSEUDOBINARY MELTS

The tendency of a supercooled pseudobinary melt $A_xB_{1-x}X_2$, where A and B are isoelectronic cations, to undergo $A \to B$ or $B \to A$ substitution can be expected in general to be high near $x \cong 0$ and $x \cong 1$. This is driven by entropic considerations to the Gibbs free energy

$$G = U - TS \,, \tag{4}$$

where one picks up the entropy of mixing when $A \to B$ or $B \to A$ substitution occurs near the end compositions and lowers the Gibbs free energy of the alloy system. As x increases (decreases) above (below) some threshold value x_l (x_h), enthalpic considerations become important. Strain energy can be expected to increase with x not only because of differences in local bonding requirements, such as differences in atomic sizes of the cations (A,B), but also because of differences in their nonlocal bonding requirements, such an an affinity for forming edge versus corner sharing tetrahedra. These considerations will generally result in the tendency of the alloy to phase separate into characteristic clusters, particularly in the middle ($x = \frac{1}{2}$) of the phase diagram. These clusters may be of AX_2 or BX_2 type, or those formed on account of a disproportionation of these parent clusters, or alternatively these clusters may be native to the disordered phase. Several factors can be identified that will induce a tendency of phase separation in rapidly cooled $A_xB_{1-x}X_2$ melts. These include the following:

(a) different melting temperatures of the end member compositions,

(b) different cluster morphologies of end member compositions, and

(c) different local and nonlocal bonding requirements of the A and B cations.

We will briefly consider two specific systems on which recent spectroscopic data reveal the two alternative examples of microstructural behavior under discussion here.

Raman vibration spectra of $Si_{1-x}Ge_xS_2$ glasses have been recently reported[3] and these, like those of corresponding crystals, show that for compositions in the range $0.05 < x < 0.80$, one can generally deconvolute these spectra in terms of local vibrational modes of characteristic SiS_2 and GeS_2 molecular cluster with relative weights determined by x. Such behavior has been interpreted in terms of two coexisting networks of separate molecular clusters. Such microscopic immiscibility or phase separation, we believe, is driven by factors (a)—(c) mentioned above. Not only are the melting temperatures[13] of the end-point members [SiS_2 (1090 °C), GeS_2 (800 °C)] widely separated, but also the cluster morphologies of SiS_2 (quasi-one-dimensional) and GeS_2 (quasi-two-dimensional) are sufficiently different to induce phase separation. Apparently the nonlocal bonding requirements of tetrahedrally coordinated Si and Ge are sufficiently different; $Si(S_{1/2})_4$ units couple more strongly to units of its own kind than to $Ge(S_{1/2})_4$ units. One notes that $Si(S_{1/2})_4$ units

will only share edges to form a quasi-one-dimensional chain as in SiS_2; $Ge(S_{1/2})_4$ units on the other hand, tend to be more flexible and share edges or corners to form a layered structure (quasi-two-dimensional) in GeS_2, for example.

Bulk glass formation in the $Ge_{1-x}Sn_xSe_2$ ternary system is known[11] to occur only in the $GeSe_2$-rich phase ($0<x<0.5$). This is because of the poor glass-forming tendency of $SnSe_2$. In the region of bulk glass formation studied[11] using Mössbauer spectroscopy, we have observed quite a remarkable x variation in the fraction T of tetrahedral $Sn(Se_{1/2})_4$ units of the network. At low x ($0<x<0.03$), T saturates at a value of 0.84, while at higher x ($0.03<x<0.45$), $T(x)$ exhibits two characteristic peaks, one centered at $x=0.07$ and the other at $x=0.35$. For convenience we have reproduced these data in Fig. 6, which is taken from Ref. 11. A model based on complete phase separation into networks of $GeSe_2$ and $SnSe_2$ clusters would require $T(x)$ to be independent of x to first order. Such an expectation is in qualitative discord with our observations. To understand the $T(x)$ data we have suggested that substantial Sn for Ge substitution occurs for $x<0.35$. This we believe to be the case because the nonlocal bonding requirements of Sn and Ge are not as different from each other as those of Si and Ge. We suppose[7] that a-$SnSe_2$ is a quasi-three-dimensional network composed of weakly interacting $Sn(Se_{1/2})_4$ tetrahedra, with density substantially lower than c-$SnSe_2$. The phase separation tendency in this system, while somewhat accentuated by the difference in covalent radii of Sn and Ge, is, however, suppressed on account of factors (a) and (c). This is the case because the melting points[14] of $GeSe_2$ (740 °C) and $SnSe_2$ (675 °C) are reasonably close to each other and also because the intertetrahedral interactions, as manifested by the bridging chalcogen bond angle θ, Ge—S—Ge, become progressively weaker as $\theta\rightarrow\pi/2$ in ascending order of the cation mass (Si→Ge→Sn).

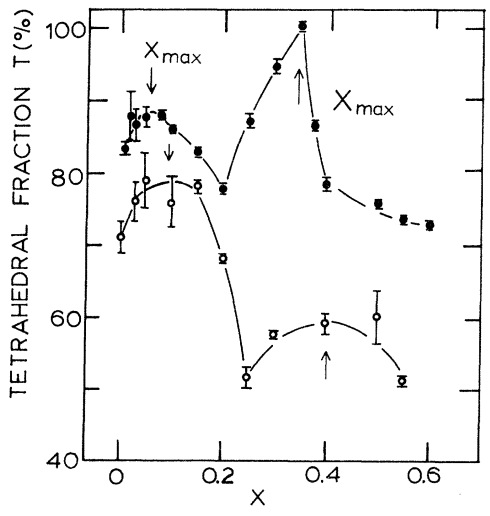

FIG. 6. Mössbauer tetrahedral Sn fraction $T(x)=I_A/(I_A+I_B)$ plotted as a function of x for $Ge_{1-x}Sn_xSe_2$ glasses (●) and $Ge_{1-x}Sn_xS_2$ glasses (○). Notice for Se-containing glasses $T=1$ at $x=0.35$ (see Refs. 11 and 12 for details).

VI. CONCLUSIONS

The crystallization behavior of ternary $Ge_{1-x}Sn_xSe_2$ glasses containing small concentration x ($0.002<x<0.01$) of Sn has been followed by Mössbauer spectroscopy. From the microscopic nature of the sites populated in the glasses as well as the crystals and particularly their x dependence, it is shown that Sn replaces Ge in the tetrahedral network of both c-$GeSe_2$ and g-$GeSe_2$. The data further show that a lower limit to the solubility of Sn in c-$GeSe_2$ is approximately 0.2 at. %, while its value in g-$GeSe_2$ is substantially higher and is conservatively placed at 3 at. %. The first crystalline phase to separate on exceeding the solubility limit in the Sn-poor regime of this ternary is shown to be c-SnSe and not c-$SnSe_2$. A parallel behavior is also observed in corresponding glasses where the first foreign phase to nucleate for $x>0.35$ as a precursor to eventual crystallization is the a-SnSe phase.[11]

ACKNOWLEDGMENTS

We are particularly grateful to Professor Kevin Sisson, George Lemon, and Wayne Bresser for assistance in data processing and to Dr. John deNeufville, Dr. M. Tenhover, and Dr. J. C. Phillips for some valuable comments during the course of this work. We are also grateful to Energy Conversion Devices, Inc. for generously providing x-ray diffraction results on our samples. This work was supported by National Science Foundation Grant No. DMR-82-17514.

APPENDIX

Lees and Flinn[15] showed sometime ago that the ^{119}Sn isomer shift (δ) in terms of the number ns (np) of $5s$ ($5p$) valence electrons of Sn can be written as follows:

$$\delta=-0.38+3.10n_s-0.17n_sn_p-0.20n_s^2\ ,$$

where δ is in units of mm/s. The shifts are quoted relative to Sn^{4+} as in $CaSnO_3$. For tetrahedral Sn (as in α-Sn) $n_s=1$ and $n_p=3$. The above equation yields $\delta=2.02$ mm/s, one of the calibration points for the above equation.

Next, one assumes that the presence of a more electronegative ligand (X) removes some of the sp^3 covalent bond charge to the ligand in proportion to the Pauling electronegativity difference $\chi(X)-\chi(\mathrm{Sn})=\Delta\chi_p$, i.e., $n_{s,p}\rightarrow n_{s,p}(1-\beta\Delta\chi_p)$. This yields

$$\delta=2.02-4.52\beta(\Delta\chi_p)-0.71\beta^2(\Delta\chi_p)^2\ ,$$

again in units of mm/s. This equation predicts a nearly linear correlation of δ with $\Delta\chi_p$, as is observed in Fig. 4. From the slope of this line, we obtain $\beta=0.21e$. This value of β is in excellent agreement with the estimate of 0.23 for this quantity deduced from Figs. 3—8 on p. 98 in Pauling's book.[6]

[1]P. Boolchand, J. Grothaus, W. J. Bresser, and P. Suranyi, Phys. Rev. B 25, 2975 (1982).

[2]D. J. Sarrach, J. P. deNeufville, and W. L. Haworth, J. Non-Cryst. Solids 22, 245 (1976).

[3]M. Tenhover, M. A. Hazzle, and R. K. Grasselli (unpublished).

[4]K. Sisson and P. Boolchand, J. Nucl. Instrum. Methods 198, 317 (1982).

[5]C. S. Kim and P. Boolchand, Phys. Rev. B 19, 3187 (1979).

[6]L. Pauling, *Nature of the Chemical Bond* (Cornell University Press, Ithaca, 1960).

[7]P. Boolchand, Mark Stevens, and John deNeufville (unpublished).

[8]P. Boolchand, J. Grothaus, and J. C. Phillips, Solid State Commun. 45, 183 (1983).

[9]B. I. Boltaks, K. V. Perepech, P. P. Seregin, and V. I. Shipatov, Izv. Akad. Nauk SSSR, Neorg. Mater. 6, 818 (1970) [Inorg. Mater. (USSR) 6, 717 (1970)]. The structure of $SnSe_2$ is CdI_2 type and is described by G. Busch, G. Frohlish, C. Hullinger, and E. Steigmeier, Helv. Phys. Acta 34, 359 (1961).

[10]P. P. Seregin, L. N. Vasilev, and Z. U. Barisora, Izv. Akad. Nauk SSSR Neorg. Mater. 8, 567 (1972) [Inorg. Mater. (USSR) 8, 493 (1972)], show that SnSe possesses a distorted NaCl structure; see H. Krebs, K. Grun, and D. Kallen, Z. Anorg. Allgem. Chem. 312, 307 (1961).

[11]Mark Stevens, J. Grothaus, P. Boolchand, and J. Gonzalez Hernandez, Solid State Commun. 47, 199 (1983).

[12]J. C. Phillips, Solid State Commun. 47, 203 (1983); J. Non-Cryst. Solids 34, 153 (1982); 43, 37 (1981).

[13]W. Pugh, J. Chem. Soc. 1930, 2370, [GeS_2 (800°C)]; F. J. Kohlmeyer and H. W. Retzlaff, Z. Anorg. Chem. 261, 248 (1950); [SiS_2 melts about 1090°C]; see also M. Hansen, *Constitution of Binary Alloys* (McGraw-Hill, New York, 1958), p. 1162.

[14]C. H. Liu, A. S. Pashinkin, and A. V. Novoselora, Dokl. Akad. Nauk SSSR 146, 1092 (1962) [$GeSe_2$ (740±5°C)]; L. Ross and M. Bourgon, Can. J. Chem. 47, 2555 (1969) [$GeSe_2$ (740°C)]; M. I. Karakhanova, A. S. Pashinkin, and A. V. Novoselova, Izv. Akad. Nauk SSSR, Neorg. Mater. 12 (8), 1486 (1976) [$SnSe_2$ (675°C)].

[15]J. K. Lees and P. A. Flinn, J. Chem. Phys. 48, 882 (1968); Phys. Rev. B 3, 591 (1971); also see P. A. Flinn, in *Mössbauer Isomer Shifts,* edited by G. K. Shenoy and F. E. Wagner (North-Holland, Amsterdam, 1978), p. 596.

[16]G. Weyer, B. I. Deutch, A. Nylandsted-Larsen, J. U. Anderson, and H. L. Nielsen, J. Phys. (Paris) Colloq. 35, C6-297 (1974).

[17]C. G. Davies and J. D. Donaldson, J. Chem. Soc. A 1968, 946.

[18]R. H. Herber, Phys. Rev. 27, 4013 (1983); see also Ref. 17.

[19]N. N. Greenwood and T. C. Gibb, in *Mössbauer Spectroscopy* (Chapman and Hall, London, 1971), p. 374.